Veðurstofa Íslands

Use of remote sensing resources to define thresholds for landslide hazards in Iceland

Talfan Barnie, Esther Hlíðar Jensen, Jón Kristinn Helgason, Eysteinn Már Sigurðsson, Matthew J. Roberts, Morgane Priet-Mahéo og Tinna Þórarinsdóttir

Greinargerð

TB/ofl/2022-01

Veðurstofa Íslands
Bústaðavegur 7–9
IS 108 Reykjavík

+354 522 60 00
vedur@vedur.is

Veðurstofa Íslands

LYKILSÍÐA

Greinargerð nr.	Dags.	Dreifing: Opin ☒ Lokuð ☐
TB/ofl/2022-01	Mars 2022	**Skilmálar:**
Heiti greinargerðar: Use of remote sensing resources to define thresholds for landslide hazards in Iceland		**Upplag:** Rafræn útgáfa **Fjöldi síðna:** 31 **Framkvæmdastjóri sviðs:** Jórunn Harðardóttir
Höfundar: Talfan Barnie, Esther Hlíðar Jensen, Jón Kristinn Helgason, Eysteinn Már Sigurðsson, Matthew J. Roberts, Morgane Priet-Mahéo og Tinna Þórarinsdóttir		**Verkefnisstjóri:** Matthew J. Roberts **Verknúmer:** 4812-0-0061
Gerð greinargerðar/verkstig:		**Málsnúmer:** 2021-0061
Unnið fyrir: Rannsóknasjóð Vegagerðarinnar		
Samvinnuaðilar:		

Útdráttur:

This research explores new opportunities provided by satellite products for the development of an early warning system for landslides in Iceland. We specifically explore the use of the soil-moisture content satellite products delivered by EUMETSAT for the support of an early warning system of landslides triggered by excess water and, in doing so, evaluate the feasibility of an operational early warning system supported by remote sensing data. Results demonstrate that (i) the soil moisture products from EUMETSAT show a clear relationship with in-situ soil moisture measurements currently made in Iceland, (ii) there is a clear relationship between elevated soil moisture detected from satellite and an increased landslide risk, and (iii) that the addition of estimates of soil moisture anomaly somewhat improves logistic models relating rainfall to landslide probability.

Lykilorð:	Undirskrift framkvæmdastjóra sviðs:
Náttúruvá, úrkoma, skriðuhætta, fjarkannanir	Undirskrift verkefnisstjóra:
	Yfirfarið af: SG

Höfundar skýrslunnar bera ábyrgð á innihaldi hennar. Niðurstöður hennar ber ekki að túlka sem yfirlýsta stefnu Vegagerðarinnar eða álit þeirra stofnana eða fyrirtækja sem höfundar starfa hjá.

Contents

1 INTRODUCTION 5
2 DATASETS AND METHODOLOGY 7
3 RESULTS 13
4 DISCUSSION 26
5 CONCLUSIONS AND FURTHER WORK 27
6 REFERENCES 29

1 Introduction

The Icelandic Meteorological office (IMO) monitors natural hazards (water, earth, and atmosphere) to assess and communicate possible risks. With our warming climate, glaciers are receding, permafrost is melting, ground is frozen for shorter periods during the wintertime and the rainfall season extends into the winter. As mountain slopes adjust to the changing conditions, the potential for landslides increases.

Landslides are one of the most hazardous natural processes in mountainous regions. They put at risk roads, urban areas, and other infrastructure (Arattano and Marchi, 2008). Comprehensive monitoring of these hazards can help prevent fatalities and mitigate socio-economic costs, including material damage and economic disruption. This realization has led to the development and setup of natural hazard monitoring systems (Arattano and Marchi, 2008; Baum and Godt, 2010; Hürlimann *et al.*, 2019; Stähli *et al.*, 2015), going from event warning systems that focus on ongoing events to early warning or forecasting systems providing more advance warning time to allow for planning and mitigation.

These systems rely on near-real-time measurements and observations, traditionally ground-based but also more recently Earth observations from satellites and predicted values from numerical models. While most landslide monitoring systems were originally based on rainfall thresholds (Tiranti and Rabuffetti, 2010), Zhuo *et al.* (2009) showed a clear correlation between soil wetness conditions and landslides, such as it could be used in an early warning system in combination with surface elevation data. Other studies demonstrate the importance of soil moisture in improving the definition of thresholds and reducing the number of false alarms (Bittelli *et al.*, 2012; Bordoni *et al.*, 2015; Brokka *et al.*, 2016; Leonarduzzi *et al.,* 2017; Hürlimann *et al.*, 2019; Marino *et al.*, 2020; Thomas, Collins and Mirus, 2019, Wicki *et al.* 2020).

As computer processing improves and remote sensing images become more freely available, these fast-developing resources are being increasingly utilized. Yet currently, satellite imaging is used typically in the aftermath of landslides to delineate inundation extent using images in the visible infrared spectrum (Cheng, Wei and Chang, 2004; Mondini *et al.*, 2011; Nichol and Wong, 2005). Therefore, this approach is dependent on daylight and cloud-free conditions to evaluate the change of slope conditions (Dabiri *et al.*, 2020; Larkin *et al.*, 2020). During the last decade, new methodologies have been developed and tested using soil moisture estimates from satellite radar images (Brokka *et al.*, 2016; Marino *et al.*, 2020) to complement or replace ground-measurements that are often sparse both in time and space and/or difficult to perform, and support landslides monitoring systems. Downscaling methods can be used to compensate for the coarseness of the soil moisture radar data (Kim *et al.*, 2018; Peng *et al.*, 2017).

Soil moisture measurements are scarce in Iceland. To date, there have been occasional studies of soil moisture for agricultural purposes (Landbúnaðarháskólinn, unpublished). The Icelandic Road and Coastal Administration (IRCA) measures soil moisture in roads, but these measurements do not represent natural conditions. Since December 2018, IMO has been running a soil moisture measuring station close to Reykjavík with the goal of detecting precipitation on frozen ground in relation to possible contamination of potable water from groundwater aquifers (Guðrún Nína Petersen, 2018). In November 2021, a soil moisture measuring station was established in Seyðisfjörður as a part of several techniques to monitor the hillside after a series of major landslides in December 2020. Large debris flows hit the town of Seyðisfjörður, resulting in the evacuation of inhabitants and considerable damage to property and infrastructure. The economic activity of the town was put to a complete stop for several days.

Studies in Iceland have shown that the main triggering factors of landslides are intense precipitation, thawing permafrost and seismic activity (Sæmundsson *et al.*, 2003; Sæmundsson *et al.*, 2018; Van Vliet-Lanoë and Guðmundsson, 2015). In recent years, recurring landslides have made the news: Móafellshyrna í Fljótum in 2012 (Sæmundsson *et al.*, 2018), Árnesfjall á Ströndum in 2014, Fagraskógarfjall (Larke *et al.*, 2020), Hleiðargarðsfjall in Eyjafjörður in October 2020, Neðri-Botnar in Seyðisfjörður in December 2020 and Útkinn in Þingeyjarsveit in October 2021. As the climate continues to warm, larger areas of permafrost will melt, thus creating conditions for landslides from high-elevation slopes. Likewise, global warming will result in more extreme and seasonally variable weather conditions, with intense rainfall being a primary trigger for landslides. Climate-change projections underline the need for comprehensive, advanced monitoring of landslide susceptibility.

Economic and human losses associated with snow avalanches and landslides have been evaluated at 13 billion ISK between 1974 to 2000 by Jóhannesson and Arnalds (2001). Since 2000, urban areas have expanded significantly, infrastructure has continued to develop, and increased tourism is creating new economic activities and overall population growth in previously isolated areas. However, monitoring of avalanches and other mass movements relies largely on analysis of meteorological conditions, observations, and experience of the terrain by experts at IMO, assisted by local contacts for landslide observations (Jensen, 2004). Events in Seyðisfjörður in 2020 changed IMO's monitoring and assessment approaches, prompting the development of a local early warning system based on various ground- and space-based measurements and forecast data. This project is an experimental contribution to this new forecasting system.

Aim

This research explores new opportunities provided by satellite products for the development of an early warning systems for landslides. The concept will be tested on selected landslides from the East of Iceland to determine if the events could have been forewarned in relation to timing and location.

The IMO and the IRCA have been working in close collaboration over the years to monitor hazards that can affect or damage road infrastructure in Iceland. This project aims at developing new tools that will ultimately improve the services of IMO to authorities such as IRCA.

This research is intended to be the starting point of a larger project to develop an early warning system for various types of natural hazards, including landslides, flash floods, snow avalanches and ice jams. Such a system would help the Icelandic authorities to monitor, detect and mitigate hazardous events. In this study, we will specifically explore the use of the soil-moisture-content satellite products delivered by EUMETSAT for the support of an early warning system of landslides triggered by excess water and, in doing so, evaluate the feasibility of an operational early warning system supported by remote sensing data.

The focus will be on three major questions:

1. Can soil moisture content products from EUMETSAT be used to improve the definition of thresholds for landslide events in Iceland?
2. Are the satellite products frequent enough to help with short to medium term advance warning prior to an event?
3. If this methodology is successful at a local level, can it be translated and used operationally in an early warning system for Iceland?

2 Datasets and methodology

Landslide observations

The Icelandic landslide database operated by the Icelandic Institute of Natural History and IMO has over 7,000 registered landslides. Many of these landslides are historical landslides with the oldest dating back to settlement times. The inventory of landslides that was selected for this project were events that occurred between 2010 and 2021 on the Eastern coastline, more specifically between Borgarfjörður Eystri in the North and Berufjörður in the South (Table 1). The focus area was between Seyðisfjörður and Eskifjörður as these areas are more prone to landslides. The selected landslides for this study only date back to 2010 due to the temporal limit of the satellites, as most platforms began to acquire observations between 2010 and 2020. Only slope failures that include debris flows, debris slides, and earthflows were selected. Rockfalls were excluded from this research as they are much harder to predict. The size and spatial distribution of the landslides differ, although in this study they are treated as having the same size, that is hit or no hit.

Table 1. Annual, cumulative number of landslides for nine locations between 2010 and 2020.

	Abbreviated locations (for explanation, see main text)									
Year	**be**	**bu**	**es**	**fk**	**ne**	**nf**	**ry**	**se**	**sy**	**total**
2010		1							1	**2**
2011		1								**1**
2013									2	**2**
2014	1		2				3	1	6	**13**
2015					1			7		**8**
2016		5								**5**
2017		1	1			1		4		**7**
2018			1					1		**2**
2019			2			4	2	1	1	**10**
2020			12	2			2	17	4	**37**
Total	**1**	**8**	**18**	**2**	**1**	**5**	**7**	**31**	**14**	**87**

In Seyðisfjörður, many landslides have occurred over the years, and it is worth mentioning the major, damaging landslides that took place in December 2020. Following these events, a dense network of instruments was setup in Neðri-Botnar area, which is above the southern part of Seyðisfjörður. Amongst other measurements, a rainfall gauge was established at 170 m above sea level, and it is used to improve information about precipitation in the area.

In-situ soil moisture measurements

Aside from specific projects by the Agricultural University of Iceland (LBHÍ) for locations such as Möðrudalur (Ólafur Arnalds and Jón Guðmundsson, personal communication), few soil-moisture instruments have been operated in Iceland. The IRCA measures moisture in roads, but these

measurements do not represent natural soil conditions so there are not applicable to landslide assessments. Since 2019, IMO has operated a soil moisture meter in Heiðmörk. Also in November 2021, a soil moisture meter and two thermometers were installed in Neðri-Botnar in Seyðisfjörður, close to the rainfall gauge that was installed in January of the same year. In summary only limited timeseries of soil moisture are available to this study.

In-situ measurements for volumetric water content are compared to satellite measurements of surface moisture level. This is not straightforward since the meter is buried at 50 cm depth, but the satellite only senses moisture level in the first 0-5 cm of the topsoil. We see that it takes time for precipitation to reach deep into the soil and changes happen with more inertia than on the surface. The approximate lag or time difference between signal on the surface and at depth is identified by shifting the in-situ measurements forward in time until they match the surface moisture. Then it makes sense to look at the data together and determine if there is a correlation between the variables. This is done by going through the satellite dataset and finding the closest matching time stamp in the in-situ dataset while accounting for time lag and comparing the two variables.

Precipitation measurements

Precipitation measurements were used for comparison with in-situ soil moisture observations, comparison with operational satellite soil moisture observations received at IMO, for comparison with historical satellite soil moisture data, as well as to calculate the Antecedents Precipitation Index (API) and to demonstrate the operation of the current landslide detection system.

Precipitation data from monitoring stations in the East Fjords and Hólmsheiði were used to analyse operational satellite data and in-situ soil moisture measurements. A precipitation station in the town of Seyðisfjörður, with an automatic precipitation monitoring has been in use since 1995. Measurements from the two collective stations are used in this study, forming a composite time-series from 1995 to 2021. The recent precipitation station in Botnahlíð improves the data series even further. So far landslide events cannot be linked to in situ soil moisture data. The measurements from Seyðisfjörður only reach back to November 2021. A precipitation gauge at Hólmsheiði east of Reykjavík has useable time series from the year 2008. This site is used for comparison with soil moisture measurements in Heiðmörk.

For the comparison with historical satellite data, precipitation data for the study area (green polygon in Figure 1) was taken from the automated and manual stations shown in Table 2. The data gives the total rainfall for 24-hour periods from 09:00 to 09:00 going back to 2015 for all stations except Teigarhorn, which started in 2018 and Bakkagerði which started in 2017. The average value from all stations was used for comparison with the soil moisture anomaly timeseries described in the next section. One station Hólmsheiði (no. 1481) is not within the study area, although it was used to analyse longer timeseries for API calculations. Note that the overlap between soil moisture measurements and nearby precipitation data in Heiðmörk only extends back to 2019.

The index of moisture stored within a drainage basin before a storm has been called antecedents precipitation index (API). The API is a weighted summation of daily precipitation amounts, used as an index of soil moisture stored within a drainage basin before a storm.

Table 2. Meteorological stations used in this study.

Station	Name	Latitude	Longitude
565	Svínafell	65.51348	-14.2
616	Hánefsstaðir	65.28543	-13.87152
620	Dalatangi	65.26817	-13.57593
626	Neskaupstaður	65.14967	-13.6576
666	Gilsá	64.8593	-14.23678
675	Teigarhorn	64.67614	-14.34406
1481	Hólmsheiði	64.1085	-21.6864
4180	Seyðisfjörður Vestdalur	65.28137	-14.00042
4182	Seyðisfjörður	65.25487	-14.00645
4193	Dalatangi	65.26815	-13.57497
4380	Bakkagerði	65.52352	-13.816731
5981	Eskifjörður	65.07633	-14.03695
5982	Fáskrúðsfjörður Ljósaland	64.93723	-14.0407
5990	Neskaupstaður	65.15027	-13.66942

Satellite data

Overview

Changes in the physical properties of soil and vegetation brought about by changes in soil moisture can be detected by satellite-borne instruments operating across the electromagnetic spectrum. When choosing the instruments with which to monitor soil moisture for landslide prediction at high latitudes several requirements need to be taken into consideration, principally:

(1) Reliability under a range of illumination conditions, including low light levels and low illumination angles in winter, and preferably at night.
(2) High enough spatial resolution to allow soil moisture variability to be monitored at a spatial scale useful for prediction.
(3) High enough frequency to track changes on a timescale of individual weather systems and provide advance warnings of landslides.
(4) A long and consistent data archive that can be used to establish empirical relationships between soil moisture and landslides.
(5) Reliable even in conditions of total cloud cover.

The latter requirement is particularly important in Iceland given the high number of cloudy days during the year, and the domain of application, as landslides tend to take place during or shortly after periods of heavy rainfall. This sets this application apart from other remote sensing studies of soil moisture that tend to focus on early detection of drought conditions (Ford and Quiring 2019).

Several different approaches have been developed for characterising soil moisture using visual to shortwave infrared (SWIR) wavelengths. In the SWIR, the presence of soil moisture leads to a decrease in reflectance (the "darkening effect" noted by Sun *et al.*, 2021) and changes in plant phenology, such as drought conditions that can be detected by changes in the "red edge" spectral feature in the red-near infrared region (as typically tracked by the Normalised Difference Vegetation Index, or NDVI, e.g. Karnieli *et al.,* 2010). Sensors operating at these wavelengths have high resolutions and short repeat times (although there is some trade-off between the two), however they are more suitable for bare soil conditions, or situations where the relationship between plant phenology and soil moisture is well established. They also cannot be used at night or, crucially, during cloudy conditions, so they were not considered further. Similarly, instruments at the thermal infrared wavelengths can pick up changes in thermal inertia and the amplitude and phase of the diurnal surface temperature cycle brought about by the impact of water's high heat capacity and latent heat flux on the thermal balance of the soil (see Zhang and Zhou, 2016 for a review). These sensors do work at night, but they also tend to have a lower spatial resolution and are again affected by cloud cover, so they too were also not considered for this project.

Having ruled out the visible, shortwave, and thermal infrared bands, we are left with microwave instruments. In the microwave region changes in soil moisture can result in substantial changes in the properties of the soil that govern its interaction of electromagnetic radiation. For instance, changes in moisture content can change the dielectric constant from around 80 to ~3–4, resulting in emissivity changing from ~0.95 to ~0.6 which will change thermal emission for a given temperature (Schmugge, 1980), as well as change the backscatter coefficient, which affects how the surface reflects incoming microwaves. Microwave sensors also have the advantage of operating at night, and through cloud and, therefore, they have been used to study soil moisture patterns at a global scale since the launch of the SMMR instrument on Nimbus 7 in 1978 (Owe *et al*., 2008), and operationally produced soil moisture products are produced in near real-time and made available by various satellite data providers.

Microwave sensors

Microwave instruments come in two types, passive instruments which measure the thermal emission from the Earth as a function of surface emissivity and temperature, and active instruments that emit microwaves and measure the energy returned from the surface, which is a function of the backscatter coefficient of the surface. The natural thermal emission from the Earth surface is very weak in the microwave, requiring integration over a large area for a reasonable signal to noise ratio, resulting in passive microwave sensors having the lowest spatial resolutions of all sensors under consideration, typically on the order of tens of kilometres. In contrast to passive sensors, active instruments emit radiation and measure the signal returned to the sensor from the surface. These sensors can be further sub divided into Synthetic Aperture Radars (SAR) and scatterometers. SAR sensors simulate a larger antenna by combining multiple observations of the same target along their orbit, resulting in a much higher spatial resolution, on the order of meters, while also measuring the phase of the returning signal for interferometry applications. However, they tend to have smaller swath widths and longer revisit times, hence not being employed for soil moisture studies to date. The other type of active sensor, scatterometers, are optimised for very precise measurements of backscatter to within a tenth of a decibel for measuring windspeeds over oceans, and therefore still need to integrate energy over a wide area, resulting in spatial resolutions like those of passive sensors on the order of tens of kilometres (Frison *et al.*, 2016).

The lower resolution passive radiometers and scatterometers have wide swath widths and therefore low revisit times typically on the order of one to three days. The main passive sensors currently in operation are the Soil Moisture and Ocean Salinity (SMOS) mission operated by ESA, with a ~43 km resolution, maximum revisit time of ~3 days and an archive extending back to March 2016 and

Soil Moisture Active Passive (SMAP) with a 36 km resolution, a revisit time of ~1 day and an archive extending back to March 2015, while the Advanced Scatterometer (ASCAT) operated by ESA/EUMETSAT has a resolution of ~25 km, a repeat time of 1 to 2 days. Soil moisture is typically reported as either an arbitrary Soil Water Index (SWI), or as saturation percentage (from 0 to 100), which can be converted to a volumetric ratio in units of cm^3/cm^3, if soil porosity is known. These measures of soil moisture estimates are only valid for the upper 3–5 cm of soil. Some data products come with useful flags for standing water, frozen ground, and snow.

In comparison the use of SAR sensors for soil moisture studies is still in its infancy, and few operational products are available. Some operational products such as the Disaggregated ASCAT soil moisture product use SAR data to enhance the resolution of low-resolution images, but this is using historical SAR data – the SAR images do not provide dynamic information about soil moisture changes, rather they are used for characterising static properties of the surface as expressed in the microwave and "downscaling" coarser resolution data appropriately. The SMAP mission was designed with both passive and active sensors to leverage the sensitivity of a passive microwave radiometer with the resolution of a SAR instrument, such that SAR data would be used to dynamically monitor soil moisture. Unfortunately, the SAR instrument failed early in the mission, and only conventional passive radiometer derived data products are produced operationally at the time of writing. Despite this setback, there has been renewed interest in SAR based soil moisture products in recent years, and a product based on the Sentinel 1 SAR instrument is now made available by the EU's Copernicus project with a spatial resolution of ~100 m. This does not cover Iceland at the time of writing, although a global dataset is under development. The algorithm that retrieves the soil moisture from the Sentinel 1 images is comparatively simple (a basic time series analysis that assumes short term variations in backscatter are due to soil moisture variability rather than plant phenology) and a version of it could be implemented locally at IMO, but it was found to be sufficiently time consuming to be out of the scope of this project. Consequently, we discounted the use of SAR images for an operational system at IMO as it is presently too complex and costly, although we note that this may change in the future.

After this process of elimination, we are left with soil moisture products from passive radiometers and scatterometers as our principal source of satellite data. The main disadvantages of these products are comparatively short archives, a poor spatial resolution, some gaps in the data of up to a few days, and soil moisture retrievals limited to the upper few centimetres. A few methods have been developed to work around these limitations:

(1) Improve time series length and fill gaps with composite datasets: Composite datasets can be generated by integrating and standardising data from multiple sensors, resulting in much longer datasets – for instance the Copernicus Land Service Soil Moisture ECV dataset extends back to 1978 with one estimate a day.
(2) Improve spatial resolution with downscaling / disaggregation, for instance Disaggregated soil moisture from ASCAT, downscaled using old ENVISAT SAR data, 1 km resolution, 2010 to present.
(3) Estimate soil moisture at depths greater than a few centimetres and fill in gaps using data assimilation. For instance, ECMWF land-surface data assimilation system integrates multiple sensors, models four different soil levels, extending the daily record back to 1992. NSIDC surface and root zone soil moisture, 9 km resolution, every three hours.

These enhanced datasets, along with the raw soil moisture retrieval data based on the native capabilities of the sensors are available from several data providers. When choosing which dataset and data provider to use the principal consideration is frequency and timeliness – the data needs to be available ideally daily with lag on the order of hours for it to be useful for advance warning of landslide risk, which rules out some providers. For instance, the Copernicus Land Service Soil

Moisture ECV which is based on assimilation of satellite data, despite having favourable spatial and temporal resolutions, is updated on a ten-day cycle with a ten-day latency (for the ICDR product) and so is of no use for an operational forecasting system. At IMO most satellite data is received over EUMETCAST, the European Organisation for the Exploitation of Meteorological Satellites (EUMETSAT) direct broadcast system – satellite data is received by EUMETSAT, processed, encoded into a DVB signal, transmitted to a geostationary telecoms satellite, and then broadcast over Europe. The signal is received at IMO and decoded into different datasets, resulting in data being received and decoded at the institution with a minimal delay – for instance, the delay the time from image acquisition to a processed data product being made available to forecasters at IMO can be as a short as ten to fifteen minutes. The basic soil moisture data products available over EUMETCAST are ASCAT and SMOS products, with two enhanced ASCAT products available, one disaggregated using historical SAR data to 1 km resolution, and one assimilation product that provides daily soil moisture estimates for four soil horizons. These datasets are available in a timely manner with a minimal lag between acquisition and transmission over EUMETSAT.

The selected satellite data products

For the website demonstrating the use of the operational NRT data from EUMETSAT we chose to use the basic ASCAT soil moisture product. The surface soil moisture estimate is derived from the Advanced SCATterometer (ASCAT) instrument that is carried onboard Metop-B and Metop-C polar orbiting satellites. This product provides an estimate of the water content of the 0-5 cm topsoil layer, expressed in degree of saturation between 0 and 100 [%]. The algorithm used to derive this parameter is based on a linear relationship of surface moisture and scatterometer backscatter. The data is not affected by weather or day / night conditions and a full coverage for Iceland can be expected on average once per day with a minimum time delay.

However, accessing historical data for modelling the relationship between soil moisture and landslides is difficult, because much of the data is archived by orbit, with limited subsetting capabilities. We are in contact with EUMETSAT to find a way to download long time series of data covering a small data without downloading prohibitively large volume of data, but for the time being we are forced to use more readily accessible archives for historical analyses. For this we turned to Google Earth Engine, which is a web service enabling the user to query hundreds of remote sensing and climatological datasets. Unfortunately, no EUMETCAST satellite based soil moisture products are available on Google Earth Engine, at the time of writing, however the NASA-USDA Enhanced SMAP Global Soil Moisture Data, which is a product of assimilating SMAP data into a simple two layer model of the soil, is available, and is similar to the ASCAT Root Zone Soil moisture dataset available over EUMETCAST (albeit with a higher resolution), so we are confident the analysis here can be applied easily to archived EUMTCAST data once we have access to it. We used the Soil Surface Moisture Anomaly (SSMA) dataset, which is the anomaly in moisture in the upper soil level in the model compared to climatology from a 31-day moving average of the whole dataset.

Despite being comparatively high resolution for a satellite-based soil moisture product at 10 km, the spatial resolution was still arguably too low for resolving spatial relationships between soil moisture and landslides, so we opted for a timeseries based approach. A timeseries of the SSMA was extracted from the entire dataset (which extends back to April 2015), by digitising a region encompassing all known landslides in the study area, and then finding the average value within that shape for each day (Figure 1). Missing days in the resulting timeseries were linearly interpolated.

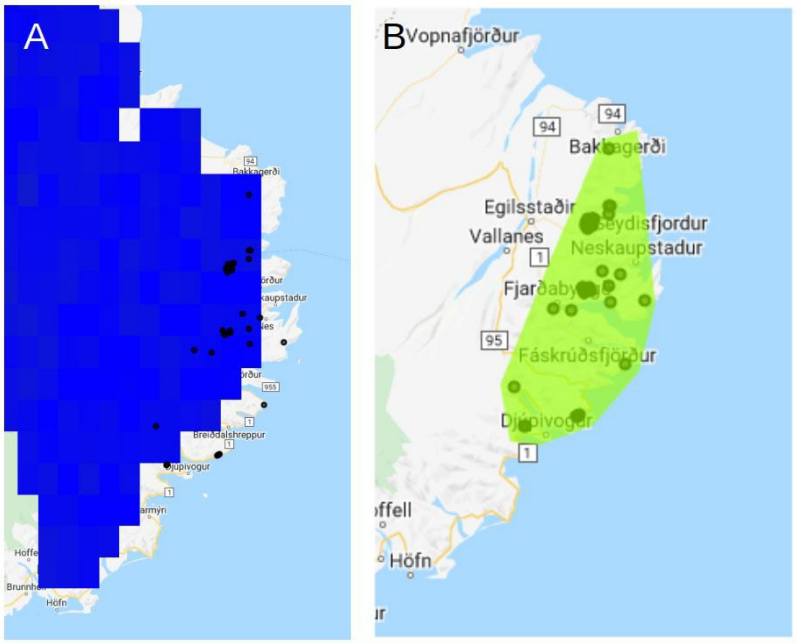

Figure 1. The study area. (A) Example NASA-USDA Enhanced SMAP Global Soil Moisture Data Soil Surface Moisture Anomaly (SSMA) image. Note the coarse 10-km resolution and clipping of the dataset. Landslide locations are shown as dots. (B) The study area outlined in green over which SSMA was averaged.

3 Results

IMO operates multiple processing chains and branches for satellite data retrieval and processing. An additional branch was set up with operational purpose in mind for this project, and now the latest ASCAT soil moisture data products are used internally at IMO. The system takes the 25 km soil moisture product that is received by direct broadcast from EUMETCAST, decodes it, and stores it in a MapServer database, which is served as Web Map Service (WMS) to internal system, forecasters and other users and displayed in a leaflet map on a webpage (Figure 2). Processing is handled by Satpy, an open-source Python library that is used to decode, reproject, and create RGB composites from various satellite sensor data. ASCAT data was not originally supported by the library, but some effort was put into writing extensions that was then contributed to the Satpy project to make it more accessible to us and others to work with soil moisture data.

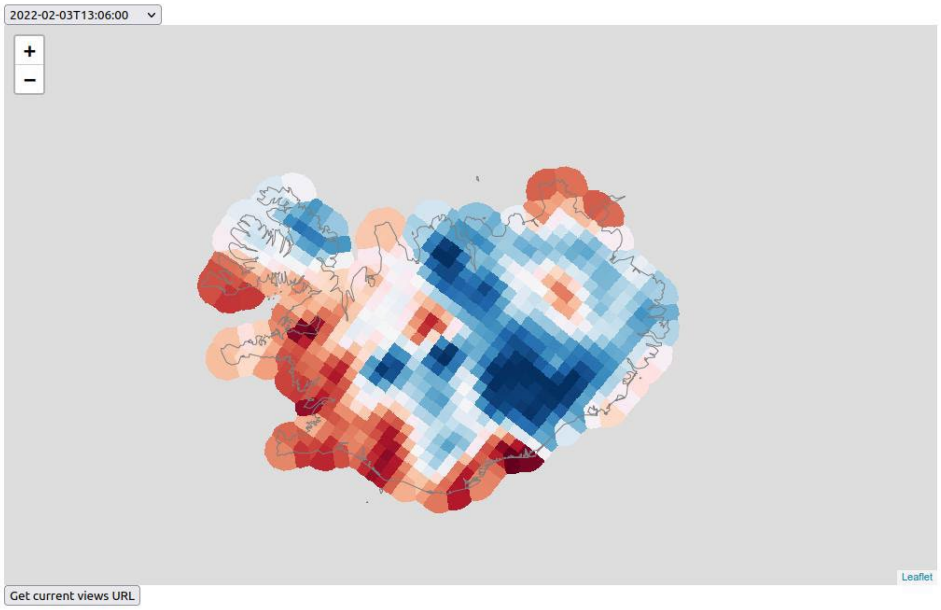

Figure 2. Example ASCAT Soil Moisture product with a resolution of 25 km, received at IMO via EUMETCAST and displayed on an internally accessible website using leaflet and MapServer.

To test the validity of the MetOp ASCAT satellite data, measurements from stationary sampling station were compared to satellite data. In this experiment, the station at Heiðmörk was chosen and for each satellite overpass that contained valid data for the location of the station, a datapoint was added to a timeseries and stored. This timeseries was then compared to measurement timeseries from the station to verify correlation between the in-situ measurements and the satellite data. The main downside to this method is that we must deal with live data since historic data was not easily available and retrieval is out of the scope of this project. This means that the comparative data is limited to a little more than few weeks. Future research should include more data that also goes back in time. Another limitation is that the fundamental difference in the data that is being compared, while the satellite data represents the moisture percentage in the 3–5 cm of the top layer, the in-situ data is measuring water content for a meter that is buried 50 cm into the soil. Despite these complications this will still give valuable insight into correlation of measurements and satellite data.

When plotted together, a relationship can be seen although the in-situ measurements seem to lag a little behind the satellite soil surface moisture observations which also exhibit more sudden changes. The lag is estimated to be around 10 hours (Figure 3). This feels like a true representation of reality since the meter is buried into the soil while the satellite observes the surface moisture only. Precipitation first falls on the surface before being absorbed into the ground layer which also has more inertia and therefore changes more slowly.

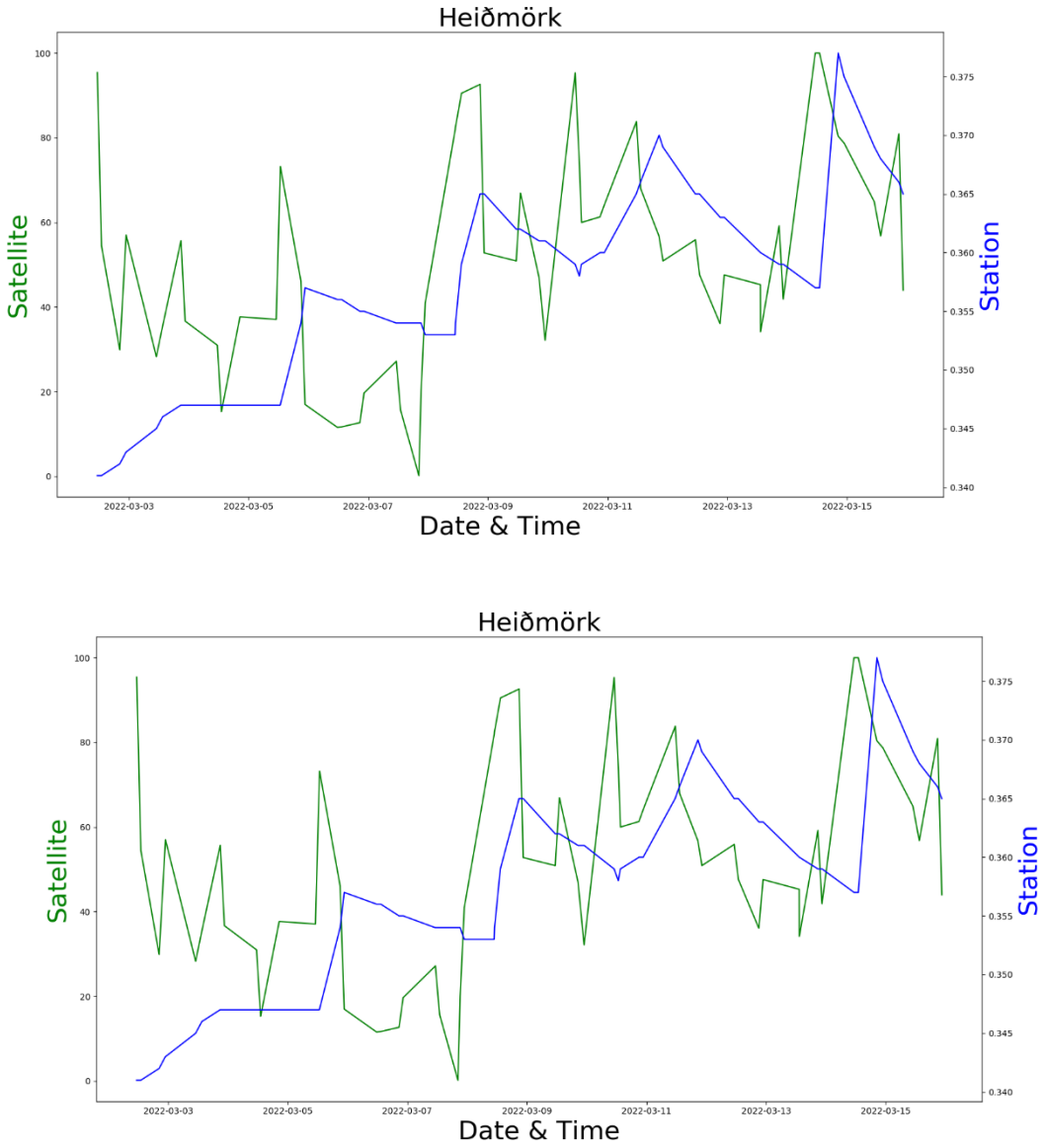

Figure 3: Above is the combined plots for satellite data and measured data at Heiðmörk, the lag can clearly be seen. Below is the same data but station data has been corrected for 10-hour lag to show the alignment of peaks.

Since the measuring station measures every 10 minutes but the satellite has only a few irregular overpasses per day, we need a method to match a timestamp for satellite data to station data. To do this, a simple Python script was developed to iterate over satellite data timeseries and match each value to the value in the measured timeseries with the closest timestamp while correcting for time lag and within reasonable time difference. This gives us two variables to compare for correlation in a scatter plot (Figure 4).

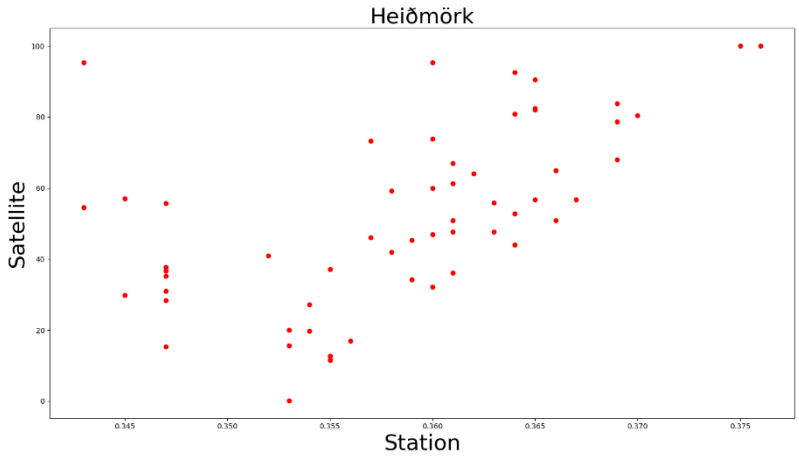

Figure 4: Measured, lag-compensated data and satellite date plotted against each other. Some correlation can be seen, despite noisy satellite data compared to in-situ data.

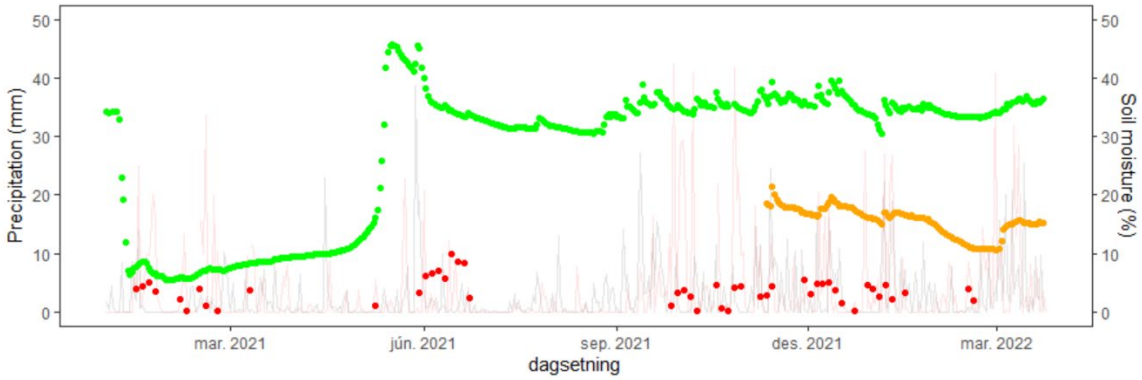

Figure 5. In situ soil moisture data from Heiðmörk (green dots), Seyðisfjörður (orange dots) and satellite soil moisture (SSMA red dots) with precipitation data in the background (pink for Seyðisfjörður, grey for Hólmsheiði).

Figure 5 shows two timeseries of monitored soil moisture in Heiðmörk and Seyðisfjörður. Even though there are only a few months shared data and about 400 km apart similar trends can be seen. We see that when there are large rainfall events (grey and pink lines) the soil moisture meters react. We also see the SSMA (note the value is calculated for the east coast of Iceland) responding to the precipitation in Seyðisfjörður.

The API index was calculated for Hólmsheiði (data series 2008–2020, Figure 6) and Seyðisfjörður (data series 1995-2020, Figure 7). Good correlation is between highest annual API values and years with landslide events in Seyðisfjörður. As can be seen in Figures 6 and 7 the API index is much higher in Seyðisfjörður than in Hólmsheiði as expected since mean annual precipitation is almost double the amount in Hólmsheiði. The high value of API in December 2020 is particularly noticeable and is much higher than ever before in the data series and linking it to the events in December 2020 gives hopes it can be used as a predictive value. The current thresholds used to issue warnings to the landslide analysts on watch is based on certain rate of annual precipitation within selected time periods (1-h, 3-h, 6-h 12-h, 24-h, 48-h, and 72-h see in more detail in discussion chapter) (Sandersen *et al.*, 1996). Analyses on the time periods and how often the thresholds have been reached gives an idea of how to link the data (Table 3).

Table 3. Date and amount of rainfall (in mm) where 24-h, 28-h and 72-h thresholds were reached in Seyðisfjörður, and if it resulted in a landslide or not. API values for comparison. Landslides are marked yes/no but in two incidents the landslide occurred the day before the 48h and 72h thresholds were reached.

Date	24h p	48h p	72h p	API	Landslide
11.9.1998	117			180	no
1.10.2001	148			232	yes
11.11.2002	160	174		314	yes
1.12.2002	0	160		323	yes
10.10.2009	129			203	no
26.8.2015	76	169		185	no
23.6.2017	164	180		255	yes
25.6.2017	1	165		259	yes-1d
18.12.2018	66	159		315	yes
24.10.2020	108			227	no
15.12.2020	171	172		460	yes
17.12.2020	140			635	yes
19.12.2020	4	145	238	666	yes-1d
28.12.2020	7	177		463	no

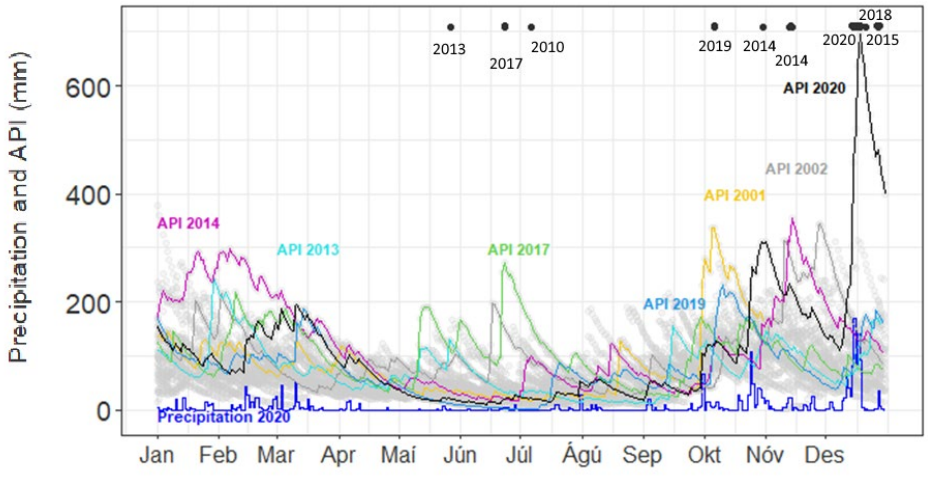

Figure 6. Precipitation (dark blue line) and API from 1995 (grey dots) and coloured lines to draw out specific years (pink, green, light blue, cyan, magenta, yellow, grey, and black) with landslide events (black dots and year plotted next to it) in Seyðisfjörður.

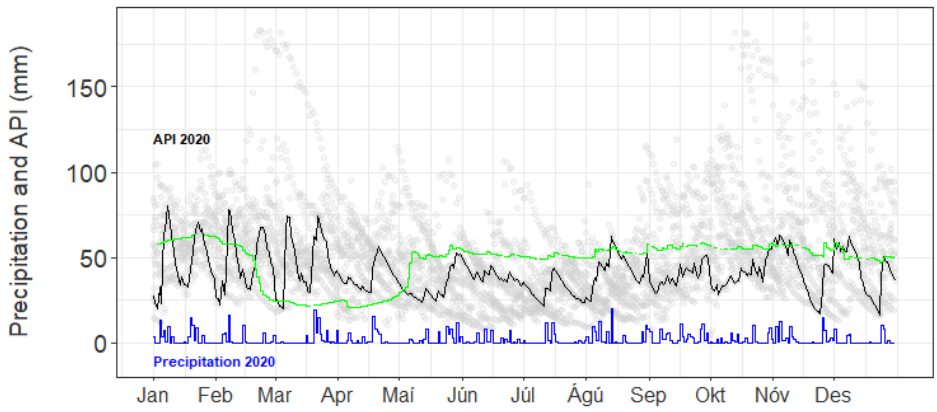

Figure 7. Precipitation (dark blue line) and antecedent index from 2008 (grey dots) and black line for API in 2020 from Hólmsheiði. Green line shows in situ soil moisture for 2020 from Heiðmörk (the measured value is exaggerated by 50%).

The analysis of historical data is shown in Figure 8. In this analysis each day has a single SSMA value, a single mean rainfall value, and a landslide code of 0 for no landslides and 1 for one or more landslides. Plotting both timeseries and marking the landslides (Figure 8a,b) shows landslides are distributed throughout the study period, while wrapping the data by year shows an absence of landslides for the first three months of the year, and the highest incidence in the last two months (Figure 8c,d). SSMA shows some seasonality (Figure 8c), with the highest and lowest anomalies appearing in the summer months, but overall, both timeseries do not show pronounced seasonality, and so this was excluded from consideration for time series modelling. Wrapping both timeseries by landslide shows the trends leading up to and immediately after a landslide (Figure 8 e,f), and reveals that on the day of a landslide both SSMA and rainfall are typically high, and while rainfall usually increases in the run up to the day of the landslide, SSMA sometimes increases and sometimes has remained elevated for some time prior to a landslide. Another way of visualising whether days with landslides are different to normal days is to compare histograms of SSMA and rainfall for days with landslides and days without (Figure 8 g,h). Here we can see that landslides only occur on days with positive SSMA values, while days without landslides range across the full range of SSMA values, from –3 to 1. Landslides occur on days with rainfall values spanning the whole of the observed range. We can get a better idea of the exact relationship between each of the timeseries and landslides by plotting the ratio of days with landslides to total days within bins of SSMA and rainfall, effectively finding the ratio of the histograms discussed previously (Figure 8i,j). For negative SSMA, there are no observed landslides, and then the fraction of days with landslides increases linearly for positive values, although the fractions remain very small. For rainfall, the fraction of days with landslides increases across the full range of observed rainfall, with landslides occurring on the rainiest days recorded. To get a continuous estimate of landslide probability as a function of these datasets we can fit a logistic model, which we do separately for SSMA and rainfall in Figure 8 k,l. Both models show an increasing probability of a landslide with increasing values, however while landslides become almost certain for very high rainfall values, the probability of a landslide as a function of SSMA does not exceed ~4%.

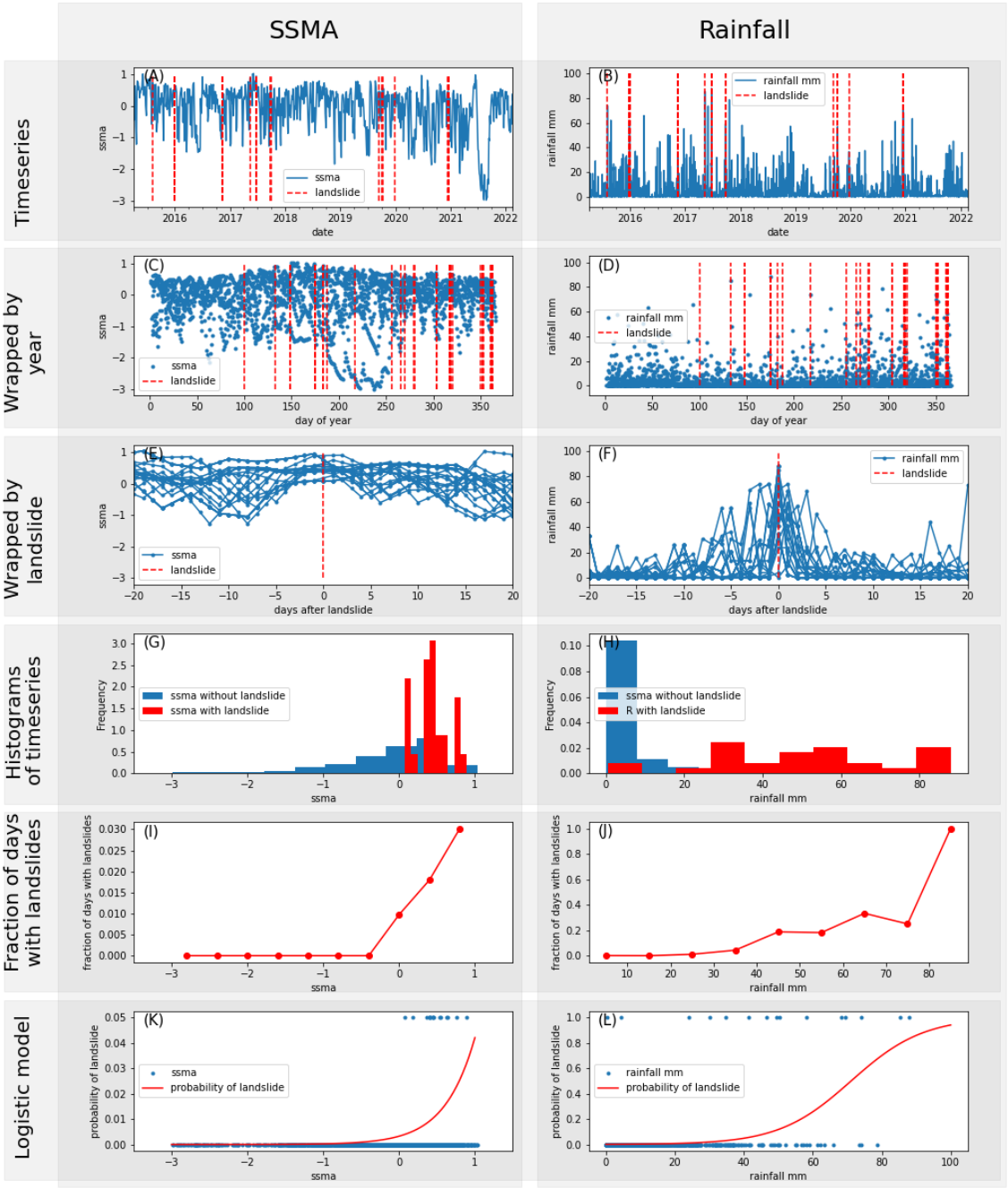

Figure 8. Overview of comparison between SSMA, rainfall and landslide data. The grid is arranged such that left and right columns show the analysis for SSMA and rainfall, respectively, while each row shows a specific analysis applied to both datasets separately. (A, B) The whole timeseries of SSMA and rainfall data, with landslides marked as vertical dashed lines. (C, D) The data wrapped by year to show any seasonality present in the data. (E, F) The data wrapped by landslide to show trends in SSMA and rainfall in the run up to, and immediately after a landslide. Time on the x axis is given as days after landslide. (G, H) Histograms comparing SSMA and rainfall on days without landslides (blue) and days with landslides (red). Note that the histograms are normalised so that the "days with landslides" histogram, which has very few days in it, is visible. (I, J) Ratio of number of days with landslides to total number of days for bins of SSMA and rainfall. (K, L). Logistic model fit to the SSMA and rainfall data.

To summarize, we can say that rainfall serves as a much better predictor of landslides than SSMA. However, so far, we have considered the SSMA and rainfall timeseries in isolation – both datasets combined may give better fit. Plotting rainfall against SSMA (Figure 9) shows that while landslides occur across the full range of observed rainfall, they do not occur for negative SSMA values. In this way, adding SSMA to the model should result in more accurate probabilities, as days with low rainfall onto dry ground will be discounted, so while rainfall would remain the main predictor for landslides, it seems likely SSMA would be a useful supplement providing more information.

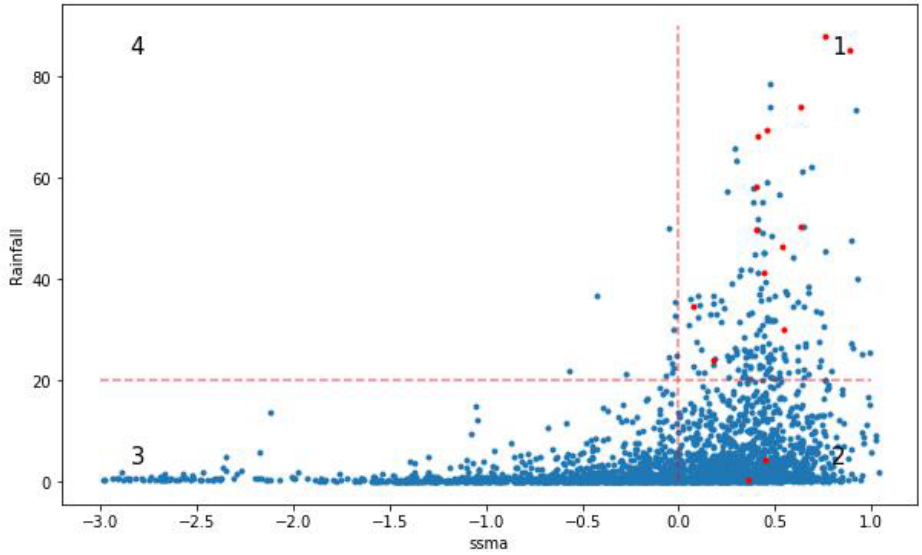

Figure 9. Plot of SSMA against rainfall for days without landslides (blue) and days with landslides (red). We divide the spaces of SSMA-rainfall into four conceptual quadrants, (1) positive SSMA, high rainfall, comparatively higher chance of a landslide, (2) positive SSMA, low rainfall, comparatively lower chance of a landslide, (3) negative SSMA, low rainfall, negligible chance of a landslide, (4) negative SSMA, high rainfall, very rare scenario, chance of landslide unknown.

We compare this joint SSMA+rainfall model with the two datasets treated separately in table 1, which shows the false positive and false negative rates, as well as the proportion of landslides missed. Note that with a threshold of P=0.5 for a positive prediction, the SSMA alone model makes no positive predictions (as the probability never gets above 0.05, see Figure 3k). Overall, the addition of SSMA timeseries to the rainfall model does not improve the model performance, which is quite poor overall, with a 50% false positive rate and 80% of landslides being missed.

Table 4. Assessment of logistic regression of landslide data against the timeseries, alone and in combination. The threshold for prediction of a positive event was taken as P=0.5.

Statistic	SSMA	Rainfall	SSMA +rainfall
Proportion of positives that are false	na	0.5	0.5
Proportion of negatives that are false	0.0060	0.0048	0.0048
Proportion of landslides missed	1.0	0.8	0.8

However, for an operational system, we could choose any threshold probability for triggering a warning. The exact threshold chosen defines the proportion of true and false positives and negatives that the system will generate. By iterating over thresholds from 0 to 1 and calculating the True Positive Rate (TPR, true positives divided by total positives) and False Positive Rate (false positives divided by total positives) from the historical data, we trace out a curve in TPR-FPR space that shows visually the trade-off between the two for a given model. This is known as the Receiver Operating Characteristic (ROC) curve, as shown in (Figure 10a), where each model under consideration (rainfall, SSMA, and rainfall and SSMA combined) defines a separate curve. Repeating this process for the False Negative Rate (FNR, false negatives divided by total negatives), and False Positive Rate (false positives over total positives) gives the Detection Error Trade-off (DET) curve, shown in Figure 10b. The Area Under Curve (AUC) value, which is simply the integral of the ROC curve gives an estimate of the performance of a model – an ideal model as an AUC of 1, as the TPR is 1 for all thresholds above 0 for a model that always gives true positive predictions, with less than idea models have an AUC below this. The combined model (SSMA+rainfall) has a slightly higher AUC value, and therefore we can say it does perform slightly better. For this model, the ROC curve shows we can get up to a TPR of ~0.85 while keeping the FPR below 0.1, after which the latter starts rising rapidly. However, the DET shows there is no threshold that gives a FNR of below 5%.

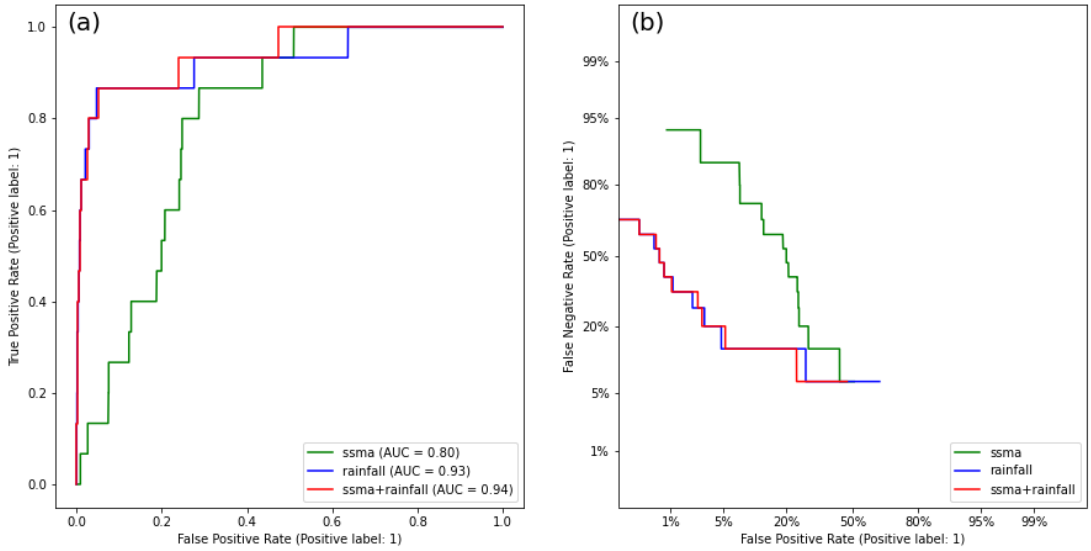

Figure 10. (a) Receiver Operating Characteristic (ROC) curve and (b) Detection Error Trade-off (DET) curve for the three logistic models: SSMA, rainfall, and rainfall and SSMA combined. Note the nonlinear x and y scales of the DET curve.

In the preceding analysis we have focussed on discrete model predictions (either a landslide occurs, or it does not, based on the probabilities output by the model relative to some threshold), but it is useful to look at the output model probabilities themselves to see if they make sense, as these raw values are useful for more detailed hazard assessments; for instance, to see how probability compounds over longer periods. A good way to assess their validity is using a calibration plot, as shown in Figure 11a. The time series of landslide probabilities output by each model are binned by probability, and then within each bin the mean model probability and the fraction of actual landslides that occurred on those days are calculated. For an ideal model, plotting these values against each other should give a straight line through the origin of slope 1, which is to say that when the ideal model gives a 10% probability of a landslide, landslides happen 10% of the time, when the model gives a probability of 20%, landslides actually happen 20% of the time, and so on. Models with a finite amount of data will show a trend oscillating about the 1:1 relationship due to random affects, but systematic deviation from the 1:1 relationship indicates some bias in the model. For our three logistic models, we can see that the SSMA model never gives any high probabilities, so only one point is visible for the origin, while for rainfall and rainfall+SSMA, there is a lot of noise due to the small number of positives in the dataset, but not much obvious bias, or difference between the two.

In Figure 11b we show the landslide probabilities output by each model as histograms, with a logarithmic y scale to make the small number of high probabilities visible. An ideal model here looks like two peaks at either end of the x axis, one at p=0 and one at p=1, as an ideal model only makes perfect predictions (i.e., there definitely will be or won't be a landslide). Here we can see that the probabilities from the SSMA model are all below ~0.05 while the rainfall and rainfall+SSMA model have a long tail with a few probabilities up to ~0.8. However, it is not obvious if the addition of the SSMA data makes the joint model look more like the ideal model. Figure 11c shows the same histograms but zoomed in on low probabilities and with a linear y scale to investigate the bulk of the distribution, revealing how the addition of SSMA to the rainfall model increases the number of very low probabilities, showing that it is having the effect of lowering probabilities on very dry days, as we anticipated earlier.

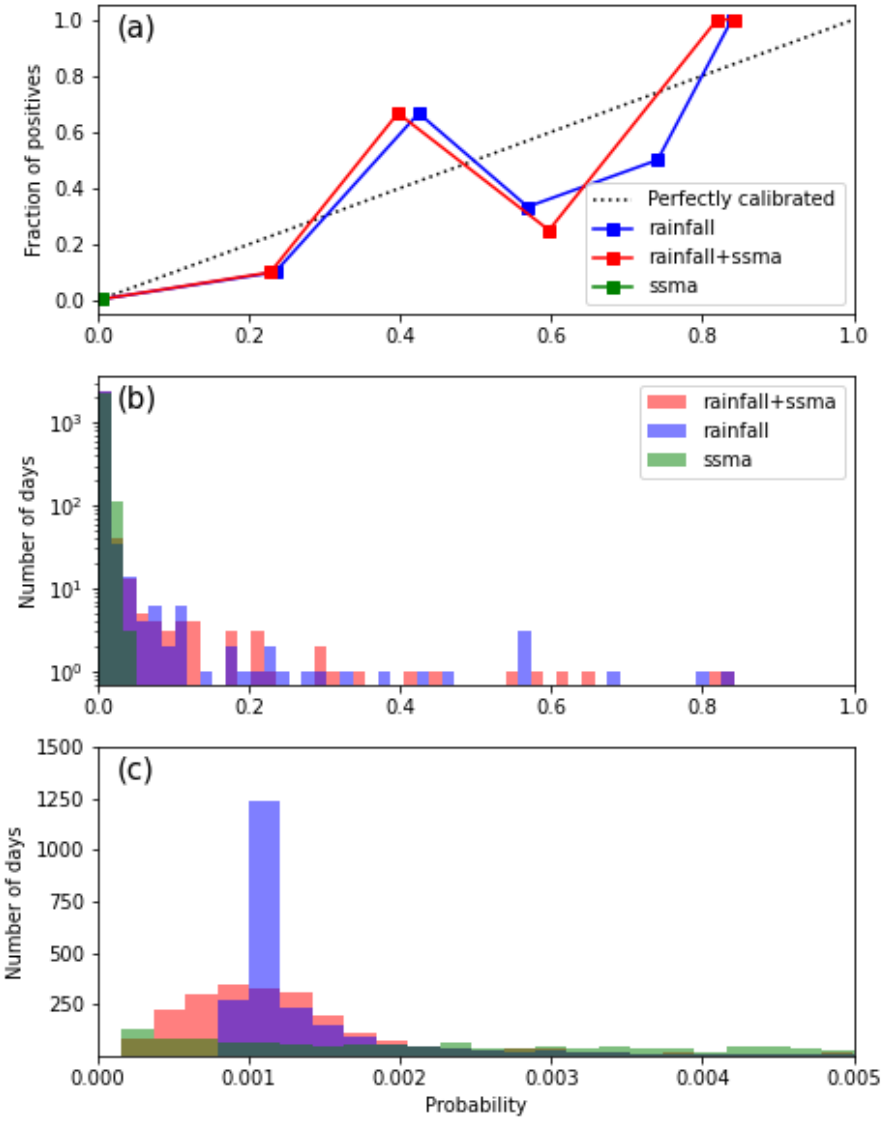

Figure 11. (A): Calibration plot for the three different logistic models, showing the fraction of landslides that occurred for bins of forecast probability. For an ideally calibrated model, landslides will occur 20% of the time the model predicts a landslide with 20% probability, 30% of the time the model predicts a landslide with 30% probability, etc. This ideal relationship is given by the grey line. Small datasets will scatter around this line due to the large effects of chance on a small sample size, but systematic offsets are indicative of a poorly calibrated model. (B): histograms of all predicted landslide probabilities for the SSMA, rainfall, and SSMA+rainfall models respectively. Note the logarithmic y scale – most of the landslide probabilities are very low. An ideal model would have two peaks at probabilities of 0.0 and 1.0 and nothing in between – i.e., all days with landslides would have a probability of 1.0 for a landslide and every day without a landslide would have a landslide probability of 0.0. (C): the same histograms but plotted with a linear y scale and the x scale zoomed in to very low probabilities. Note the combination of rainfall and SSMA shifts.

We also desire to forecast landslides in the future rather than on the day the observations of rainfall and SSMA are made. Inspecting Figure 8e,f, the rainfall and SSMA time series seem autocorrelated, so we might expect to be able to make probabilistic forecasts of these values a few days into the

future and therefore estimate the probability of landslides over a similar horizon. To make forecasts of landslide probabilities, we implemented a full Bayesian model in the Stan probabilistic programming language. An overview of the model is shown in Figure 12. We model the timeseries of SSMA and rainfall using the Autoregressive Moving Average (ARMA) model implemented by (Alstott, 2022), and then model the landslide timeseries as a logit parameterised Bernoulli distribution (Carpenter *et al*., 2017) distributed about a linear function of the modelled SSMA and rainfall.

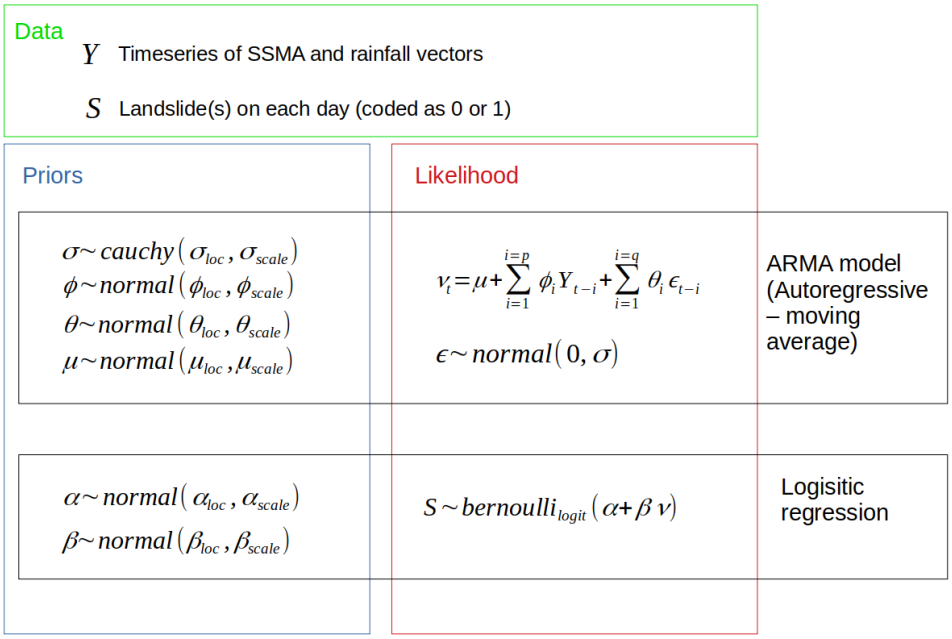

Figure 12. The Bayesian statistical model implemented in the Stan probabilistic programming language.

The model was run for 1000 samples on four parallel chains and diagnostics (effective sample size and $\hat{R}$) gave acceptable values. An example output of the model is shown in Figure 13, which shows the fit to the data for the last one hundred days of the time series, and then the forecast for the following seven days. The model describes the data well and we can make forecasts of rainfall and SSMA a few days ahead, although the quality of the forecast degrades. It should be noted that here the SSMA and rainfall are modelled as two separate timeseries, future work will model the former as a function of the latter, which will allow better SSMA forecasts, and therefore better landslide forecasts using rainfall forecasts from IMO's Harmonie numerical weather prediction mode. The model forecasts the probability of a landslide on a given day, as well as the cumulative probability of a landslide by a given day. Despite the probability of a landslide on a given day being low, cumulative probabilities have the potential to rise to high values during periods when high rainfall / SSMA are forecast. Although this model is just an early prototype, we present it here to show the types of forecasts that can be made by combining rainfall and soil moisture information with the landslide record in a Bayesian model.

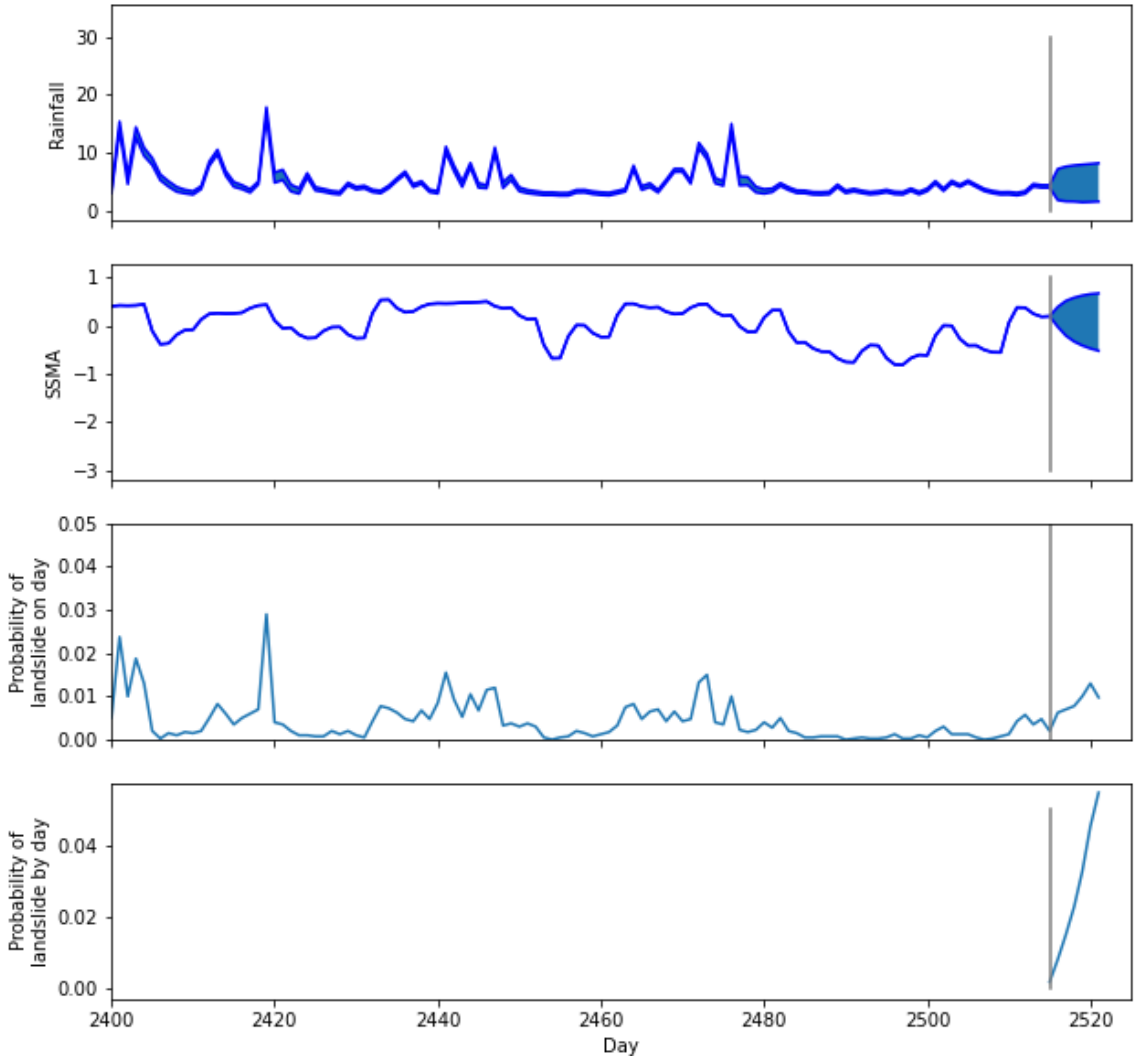

Figure 13. Example output of the Bayesian forecast model for the last one hundred days of the time series, and a forecast for the following 7 days. The top two graphs show the modelled rainfall and SSMA. The tinted area is the mean value plus and minus one standard deviation, with the plot before the grey line representing the modelled period for which data is available and the period after the grey line the forecast for the future. The lower two graphs show the probability of a landslide on a given day and probability of a landslide by a given day (i.e., the cumulative probability of a landslide having occurred by that day).

By linking the API to the soil moisture data, both in situ and satellite soil moisture the forecast model is expected to improve but with the scope of this project we did not manage to complete those calculations.

4 Discussion

Landslide early warning systems

Landslides triggered by heavy rain and/or snowmelt have been increasing in the past decades in mountainous and hilly regions around the world and due to climate change it is expected to rise even more. For the past decades the use of rainfall thresholds on regional and local scales have been used to try to forecast such events and give out warnings to the public. These methods are one of many mitigation methods available for reducing the risk of life (Picuillo *et al.*, 2019).

These systems are called landslide early warning systems (LEWS) and can be categorized into two systems that are defined by the scale of the forecasted area (Figure 14). A local system that addresses a single slope or small area are named local LEWS (Lo-LEWSs) and system that operate on regional scales or big areas are referred to as territorial systems (Te-LEWSs) (Piciullo *et al.*, 2018, Guzzetti *et al.*, 2020).

Local landslide early warning systems (Lo-LEWSs) normally operate with more instruments that monitor not just meteorological factors, but surface and subsurface conditions and deformation (Entrieri *et al.*, 2012). The systems are operationally much more complex than regional systems. After the catastrophic landslide events in the town of Seyðisfjörður in 2020, a comprehensive network was installed to monitor slope movements above a part of the settlement. It has now been operating for over a year.

Early warning systems operating at a regional scale are used to assess the probability of occurrence of multiple landslides over a predefined area. These systems most often focus on shallow landslides and are designed to forecast landslides in certain areas (Calvillo, *et al.*, 2015), regions (Baum and Godt, 2010) or even whole countries (Piciullo *et al.*, 2017), but they cannot accurately predict where the next event will occur. Typically, these systems operate on network of monitors that measure meteorological factors with the aid of historical events and precipitation to predict the probability of next event (Picuillo *et al.*, 2017).

Multiple different approaches to create precipitation thresholds have been utilized in the past. Many of them have been very successful and others not lived up to their full potential, which is often due to lack of registered events. But in recent years the focus has been on antecedent soil moisture to enhance the precipitation thresholds (Zhao *et al.*, 2019, Zhao *et al.*, 2021 and Abraham *et al.*, 2021).

The scope of this research is to enhance the regional landslide early warning system in Iceland. The current system runs on a rainfall threshold method called intensity duration (ID) design by Sanders *et al.* (1996) that have been adapted to Iceland. Threshold values that based on calculating the critical water supply as percentage of the mean annual precipitation and the duration of each precipitation event. But to improve forecasting methods the calculated threshold values for precipitation needs to be updated and include soil moisture with the aid of hydrological models and soil moisture measurements with data from in-situ instruments and satellites.

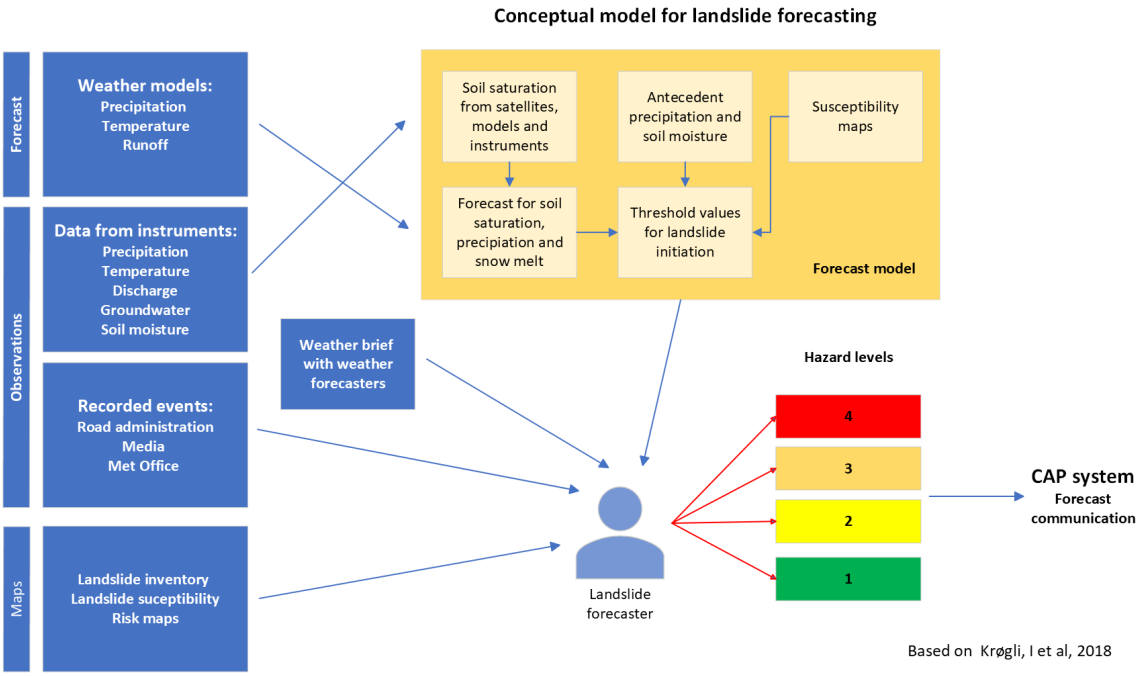

Figure 14. Conceptual model of a landslide early warning system (LEWS) that includes soil saturation. Based on Krøgli et al. (2018).

5 Conclusions and further work

In conclusion, we can address our three original questions:

(1) Can soil moisture content products from EUMETSAT be used to improve the definition of thresholds for landslide events in Iceland?

We have demonstrated that (i) soil moisture products from EUMETSAT show a clear relationship with in-situ soil moisture measurements currently made in Iceland, (ii) there is a clear relationship between elevated soil moisture detected from satellite and an increased landslide risk, and (iii) that the addition of estimates of soil moisture anomaly somewhat improves logistic models relating rainfall to landslide probability (as measured by AUC), mostly for anomalously dry days.

Many current Te-LEWs, including the system currently in operation at IMO, use API as a proxy for soil moisture, and future work could look into the possibility of combining API and satellite based estimates to better estimate soil moisture. The Bayesian model presented in Figure 12 could provide a good framework for this, allowing soil moisture to be modeled as a function of past rainfall and operational satellite products, such as from SMOS and ASCATT, both of which are available over EUMETCAST. This model could be physically based and implemented as e.g. a Kalman filter, or a basic timeseries model such as ARIMAX. Forecast rainfall from the Harmonie numerical weather prediction model could then be used to forecast soil moisture and consequently improve the forecast of landslide hazards. It is possible that API is capturing some non-soil moisture related effect of rainfall that increases landslide risk a few days after precipitation (e.g. waterlogging of vegetation), and this effect could be included by fitting the logistic model to some function of soil moisture and lagged rainfall from the previous few days. In this way the model might be considered to be implicitly finding an API optimised for landslide estimation, while also including a “best guess” of soil moisture. Such a system would need to be compared with the current API based system.

(2) Are the satellite products frequent enough to help with short to medium term advance warning prior to an event?

Given that there is a clear relationship between soil moisture, rainfall, and landslide probability, that probability can be forecast to the extent that soil moisture and rainfall can be forecast. We have demonstrated that satellite based soil moisture products are frequent enough to fit simple timeseries based forecast models for at least a short term warning.

(3) If this methodology is successful at a local level, can this methodology be translated and used operationally in an early warning system for Iceland?

We have demonstrated the potential for a combined soil moisture and rainfall based scheme for a region is Iceland. The next steps are to implement a full model and bridge the gap between the national, regional and local scales. The approach here estimates the probability of landslides over an area on the order of thousands of square kilometers. This is by necessity, as our predictor variables (rainfall, ssma) are only available at a coarse resolution or at specific point measurements, and we need to integrate over a large enough area to get a large enough sample of landslides to be able to fit a statistical model. Similar systems could be set up for other regions of Iceland, with each region of consideration delineated such as to maximize homogeneity in terms of climate and geomorphology, while remaining large enough for statistical analysis. These regional probabilities could then be "downscaled" by finding a relationship between landslide probability and geo-morphological and ecological factors (slope, aspect, soil type, vegetation type), and apportioning the regional probability accordingly at the scale common to the rasters of surface properties.

A point worth mentioning when designing an early warning system is that the analyses here are based on measured precipitation at selected stations but the precipitation from the forecasting model of the IMO; Harmonie does not always predicts the measured situation. This is especially true where the orographic effect has a great impact and the forecast model does not manage to mimic the situation. This applies to Seyðisfjörður in a certain wind direction. When moist air comes from the NA direction over Seyðisfjörður, conditions can arise where the air mass is lifted and that causes the moisture to increase and more precipitation falls than had been expected.

High spatial resolution estimates of rainfall and soil moisture would likely allow more accurate localised forecasts to be made, and such datasets will likely become available in the near future – high resolution SAR based soil moisture products are under development, and the new improved radar network being installed in Iceland by IMO over the next few years could be calibrated to estimate rainfall, however this would likely necessitate a very different approach to that taken in this study.

One further avenue of future work would be an attempt to bridge the gap between Lo-LEWSs and Te-LEWSs. In Seyðisfjörður we now have a comprehensive local monitoring system, and the detailed observations those systems will make before and during future landslides will likely inform the small scale geomorphological variables used to downscale regional scale probabilities.

6 References

Abraham, M. T., Pothuraju, D., & Satyam, N. (2019). Rainfall Thresholds for Prediction of Landslides in Idukki, India: An Empirical Approach. *Water*, *11*(10), 2113. https://doi.org/10.3390/w11102113

Alstott, J. (2022). https://github.com/jeffalstott/pystan_time_series. Accessed 31st March 2022.

Arattano, M., & Marchi, L. (2008). Systems and Sensors for Debris-flow Monitoring and Warning. *Sensors*, *8*(4), 2436–2452. https://doi.org/10.3390/s8042436

Baum, R. L., & Godt, J. W. (2010). Early warning of rainfall-induced shallow landslides and debris flows in the USA. Landslides, 7(3), 259–272.

Bittelli, M., Valentino, R., Salvatorelli, F., & Pisa, P. R. (2012). Monitoring soil-water and displacement conditions leading to landslide occurrence in partially saturated clays. Geomorphology, 173, 161–173.

Björnsson, H., Sigurðsson B. D., Davíðsdóttir B., Ólafsson J., Ástþórssson Ó. S., Ólafsdóttir S., Baldursson T., Jónsson T. (2018). Loftslagsbreytingar og áhrif þeirra á Íslandi – Skýrsla vísindanefndar um loftslagsbreytingar 2018. Veðurstofa Íslands.

Bordoni, M., Meisina, C., Valentino, R., Lu, N., Bittelli, M., & Chersich, S. (2015). Hydrological factors affecting rainfall-induced shallow landslides: From the field monitoring to a simplified slope stability analysis. Engineering Geology, 193, 19–37.

Brocca, L., Ciabatta, L., Moramarco, T., Ponziani, F., Berni, N., & Wagner, W. (2016). Use of satellite soil moisture products for the operational mitigation of landslides risk in central Italy. In Satellite soil moisture retrieval (pp. 231–247). Elsevier.

Brunetti, M. T., Peruccacci, S., Rossi, M., Luciani, S., Valigi, D., & Guzzetti, F. (2010). Rainfall thresholds for the possible occurrence of landslides in Italy. Natural Hazards and Earth System Sciences, 10(3), 447–458.

Calvello, M., 2017. Early warning strategies to cope with landslide risk. Riv. Ital. Geotec. 2, 63–69. https://doi.org/10.19199/2017.2.0557-1405.063.

Carpenter, B., Gelman, A., Hoffman, M. D., Lee, D., Goodrich, B., Betancourt, M., ... & Riddell, A. (2017). Stan: A probabilistic programming language. Journal of statistical software, 76(1).

Cheng, K. S., Wei, C., & Chang, S. C. (2004). Locating landslides using multi-temporal satellite images. Advances in Space Research, 33(3), 296–301. https://doi.org/10.1016/S0273-1177(03)00471-X Dabiri, Z., Hölbling, D., Abad, L., Helgason, J. K., Sæmundsson, Þ., & Tiede, D. (2020). Assessment of Landslide-Induced Geomorphological Changes in Hítardalur Valley, Iceland, Using Sentinel-1 and Sentinel-2 Data. Applied Sciences, 10(17), 5848. https://doi.org/10.3390/app10175848

Ford, T. W., & Quiring, S. M. (2019). Comparison of contemporary in situ, model, and satellite remote sensing soil moisture with a focus on drought monitoring. Water Resources Research, 55(2), 1565-1582.

Frison, P. L., Jarlan, L., & Mougin, E. (2016). Using satellite scatterometers to monitor continental surfaces. In Land Surface Remote Sensing in Continental Hydrology (pp. 79-113). Elsevier.

Guðrún Nína Petersen (2018). Veður í Reykjavík og á Hólmsheiði desember 2017 – janúar 2018. Technical report: GNP/2018-01. Icelandic Meteorological Office 2018. In icelandic.

Intrieri, E., Gigli, G., Mugnai, F., Fanti, R., Casagli, N. (2012). Design and implementation of a landslide early warning systems. Engineering Geology 147-148, 124-136. http://dx.doi.org/10.1016/j.enggeo.2012.07.017

IPCC (2013). Annex I: Atlas of Global and Regional Climate Projections [van Oldenborgh, G.J., M. Collins, J. Arblaster, J.H. Christensen, J. Marotzke, S.B. Power, M. Rummukainen and T. Zhou (eds.)]. In: Climate Change 2013: The Physical Science Basis. Contribution of Working Group I to the Fifth Assessment Report of the Intergovernmental Panel on Climate Change [Stocker, T.F., D. Qin, G.-K. Plattner, M. Tignor, S.K. Allen, J. Boschung, A. Nauels, Y. Xia,

V. Bex and P.M. Midgley (eds.)]. Cambridge University Press, Cambridge, United Kingdom and New York, NY, USA.

Jensen, E. H. (2004). Landslides, Hazard Assessment. Workshop "Risk mitigation of slope instability" – JRC, Ispra, It. 30. September 2004.

Krøgli, I. K., Devoli, G., Colleuille, H., Boje, S., Sund, M., Engen, I. K. (2018). The Norwegian forecast and warning service for rainfall- and snomelt-induced landslides. Nat. Hazards Earth Syst. Sci., 18, 1427–1450. https://doi.org/10.5194/nhess-18-1427-2018

Gariano, S. L., & Guzzetti, F. (2016). Landslides in a changing climate. Earth-Science Reviews, 162, 227–252. https://doi.org/10.1016/j.earscirev.2016.08.011

Guzzetti, F., Gariano, S. L, Peruccacci, S., Brunetti, M.T., Marchesini, I., Rossi, M., Melillo, M. (2020). Geographical landslide early warning systems. Earth-Science Review 200, 102973. https://doi.org/10.1016/j.earscirev.2019.102973

Hürlimann, M., Coviello, V., Bel, C., Guo, X., Berti, M., Graf, C., Hübl, J., Miyata, S., Smith, J. B., & Yin, H.-Y. (2019). Debris-flow monitoring and warning: Review and examples. Earth-Science Reviews, 199, 102981. https://doi.org/10.1016/j.earscirev.2019.102981

Jóhannesson, T., & Arnalds, Þ. (2001). Accidents and economic damage due to snow avalanches and landslides in Iceland. Jökull, 50, 81–94.

Karnieli, A., Agam, N., Pinker, R. T., Anderson, M., Imhoff, M. L., Gutman, G. G., ... & Goldberg, A. (2010). Use of NDVI and land surface temperature for drought assessment: Merits and limitations. Journal of climate, 23(3), 618-633.

Kim, D., Moon, H., Kim, H., Im, J., & Choi, M. (2018, August 27). Intercomparison of Downscaling Techniques for Satellite Soil Moisture Products [Research Article]. Advances in Meteorology; Hindawi. https://doi.org/10.1155/2018/4832423

Larkin, H., Magnall, N., Thomas, A., Holley, R., & Mccormack, H. (2020). Utilising satellite-based techniques to identify and monitor slope instabilities: The Fagraskógarfjall and Limnes landslides. Proceedings of the 2020 International Symposium on Slope Stability in Open Pit Mining and Civil Engineering, 1455–1466.

Leonarduzzi E, Molnar P, McArdell BW (2017). Predictive performance of rainfall thresholds for shallow landslides in Switzerland from gridded daily data. Water Resour Res 53:6612–6625. https://doi.org/10.1002/2017WR021044

Marino, P., Peres, D. J., Cancelliere, A., Greco, R., & Bogaard, T. A. (2020). Soil moisture information can improve shallow landslide forecasting using the hydrometeorological threshold approach. Landslides, 17, 2041–2054.

Mondini, A. C., Guzzetti, F., Reichenbach, P., Rossi, M., Cardinali, M., & Ardizzone, F. (2011). Semi-automatic recognition and mapping of rainfall induced shallow landslides using optical satellite images. Remote Sensing of Environment, 115(7), 1743–1757. https://doi.org/10.1016/j.rse.2011.03.006

Nichol, J., & Wong, M. S. (2005). Detection and interpretation of landslides using satellite images. Land Degradation & Development, 16(3), 243–255. https://doi.org/10.1002/ldr.648

Owe, M., de Jeu, R., & Holmes, T. (2008). Multisensor historical climatology of satellite-derived global land surface moisture. Journal of Geophysical Research: Earth Surface, 113(F1).

Patton, A. I., Rathburn, S. L., & Capps, D. M. (2019). Landslide response to climate change in permafrost regions. Geomorphology, 340, 116–128. https://doi.org/10.1016/j.geomorph.2019.04.029

Piciullo, L., Dahl, M.-P., Devoli, G., Colleuille, H., Calvello, M., 2017a. Adaptation of the EDuMaP method for the performance evaluation of the alerts issued on variable warning zones. Nat. Hazards Earth Syst. Sci. 17 (6), 817–831. https://doi.org/10.5194/nhess-17-817-2017.

Piciullo, L., Calvello, M., Cepeda, J.M., (2018) Territorial early warning systems for rainfall-induced landslides. Earth-Science Reviews 19. 228-247. https://doi.org/10.1016/j.earscirev.2018.02.013

Peng, J., Loew, A., Merlin, O., & Verhoest, N. E. C. (2017). A review of spatial downscaling of satellite remotely sensed soil moisture. Reviews of Geophysics, 55(2), 341–366. https://doi.org/10.1002/2016RG000543

Schmugge, T. (1980). Soil moisture sensing with microwave techniques. In Proceedings of the 14th International Symposium on Remote Sensing of Environment, 23-30 April, 1980, San Jose, Costa Rica. (pp. 487-505). Environmental Research Institute of Michigan..

Schöpa, A., Chao, W.-A., Lipovsky, B. P., Hovius, N., White, R. S., Green, R. G., & Turowski, J. M. (2018). Dynamics of the Askja caldera July 2014 landslide, Iceland, from seismic signal analysis: Precursor, motion and aftermath. Earth Surface Dynamics, 6(2), 467–485. https://doi.org/10.5194/esurf-6-467-2018

Stähli, M., Sättele, M., Huggel, C., McArdell, B. W., Lehmann, P., Van Herwijnen, A., Berne, A., Schleiss, M., Ferrari, A., & Kos, A. (2015). Monitoring and prediction in early warning systems for rapid mass movements. Natural Hazards and Earth System Sciences, 15(4), 905–917.

Sandersen F, Bakkehoi S, Hestnes E, Lied K (1996) The influence of meteorological factors on the initiation of debris flows, rockfalls, rockslides and rockmass stability. In: Senneset K (ed) Landslides. Proceedings of the 7th symposium on landslides, Trondheim, 17–21 June 1996, pp 97–114

Sæmundsson, T., Pétursson, H. G., & Decaulne, A. (2003). Triggering factors for rapid mass movements in Iceland. Debris-Flow Hazards Mitigation: Mechanics, Prediction, and Assessment, 1, 167–178.

Sæmundsson, Þ., Morino, C., Helgason, J. K., Conway, S. J., & Pétursson, H. G. (2018). The triggering factors of the Móafellshyrna debris slide in northern Iceland: Intense precipitation, earthquake activity and thawing of mountain permafrost. Science of The Total Environment, 621, 1163–1175. https://doi.org/10.1016/j.scitotenv.2017.10.111

Sun, H., Liu, H., Ma, Y., & Xia, Q. (2021). Optical Remote Sensing Indexes of Soil Moisture: Evaluation and Improvement Based on Aircraft Experiment Observations. Remote Sensing, 13(22), 4638.

Tiranti, D., & Rabuffetti, D. (2010). Estimation of rainfall thresholds triggering shallow landslides for an operational warning system implementation. Landslides, 7(4), 471–481.

Thomas, M. A., Collins, B. D., & Mirus, B. B. (2019). Assessing the Feasibility of Satellite-Based Thresholds for Hydrologically Driven Landsliding. Water Resources Research, 55(11), 9006–9023. https://doi.org/10.1029/2019WR025577

Van Vliet-Lanoë, B., & Guðmundsson, Á. (2015). Permafrost and climate change in Iceland. Environ. Périglac, 2018, 22–23

Zhang, D., & Zhou, G. (2016). Estimation of soil moisture from optical and thermal remote sensing: A review. Sensors, 16(8), 1308

Zhaou, B. Dai, Q., Han, D., Dai, H., Mao, J., Zhou, L. (2019). Probabilistic thresholds for landslides warning by integrating soil moisture conditions with rainfall thresholds. Journal of Hydrology 574, p 276-287.

Zhuo, L., Dai, Q., Han, D., Chen, N., Zhao, B., & Berti, M. (2019). Evaluation of remotely sensed soil moisture for landslide hazard assessment. IEEE Journal of Selected Topics in Applied Earth Observations and Remote Sensing, 12(1), 162–173

Wicki, Adrian, Peter Lehmann, Christian Hauck, Sonia I. Seneviratne, Peter Waldner & Manfred Stähli (2020). Assessing the potential of soil moisture measurements for regional landslide early warning. Landslides 17(8). 17:1881–1896 DOI 10.1007/s10346-020-01400-y